Partially coherent Airy beam and its propagation in turbulent media

Halil T. Eyyuboğlu · Emre Sermutlu

Abstract The properties of partially coherent Airy beam propagating in turbulent media are investigated. Firstly the variations in the intensity profile and the location of the Airy beam peak with respect to dislocation and width parameters are examined. On the source plane, it is shown that there is a threshold value of the dislocation parameter which determines whether the beam peak will lie on the negative or positive side of the axis. The changes in source beam power and source beam size with respect to dislocation and width parameters are also examined. Then analysis is made for partially coherent Airy beam propagating in turbulence against variations in propagation distance, dislocation and width parameters, structure constant and partial coherence. It is found that the peak of the Airy beam will always shift to the right for increasing propagation distance. But this shift will become less as the dislocation and width parameters are increased. Finally it is shown that higher levels of turbulence and partial coherence will lead to more spreading and shift the beam peak more toward the on-axis position.

H. T. Eyyuboğlu (✉) · E. Sermutlu (✉)
Department of Electronic and Communication Engineering, Çankaya University, Eskişehir Yolu, 29. Km, Yenimahalle, 06810 Ankara, Turkey
e-mail: h.eyyuboglu@cankaya.edu.tr

E. Sermutlu
e-mail: sermutlu@cankaya.edu.tr

E. Sermutlu
Department of Computer Engineering, Çankaya University, Eskişehir Yolu, 29. Km, Yenimahalle, 06810 Ankara, Turkey

1 Introduction

Airy functions constitute one set of solutions to the paraxial wave equation. If exponential term is excluded from the field expression, then the beam seems to have non-diffracting features when propagating in free space. Additionally, independent of the presence of the exponential term, source Airy beams have asymmetric profile with respect to the on-axis position, exhibiting a sole exponential decay for the positive values of the argument and slowly decaying oscillatory behavior for negative arguments. On the other hand, Airy beams suffer a bending to the right as they propagate. Such properties were noted by Berry and Balazs in [1] where this kind of bending was named as acceleration. Unfortunately, Airy beam composed of Airy function only possesses infinite energy and is not suitable for propagation analysis. To this end, Sivi-loglou and Christodoulides [2] have recently introduced an Airy beam model that consists of Airy function coupled with an exponential term containing the transverse plane dependence multiplied by a positive coefficient. Later Airy Gaussian beam was also proposed by Bandres and Gutierrez-Vega [3]. Calling it generalized form of Airy beams, in this work [3], the authors derived the propagation expression for an ABCD system and in particular examined the free space propagation and propagation through a graded refractive index media, also setting the conditions of square integrability, i.e. the conditions for Airy beams to have finite energy. In [4], Wigner distribution function of an Airy beam was obtained analytically, through which the weak diffraction, curved propagation and self-healing properties of Airy beams were demonstrated. Truncated and vortical Airy beams were investigated in [5] where it was mentioned that the later beams will be capable of preserving their annular structure. For strongly nonlocal

and nonlinear media, the propagation of Airy Gaussian beam was studied in [6]. Using a phase mask encoded with singularity, Dai et al. [7] carried out an experimental study on the propagation of vortex Airy beams, proving that the larger deflected velocity of the optical vortex during propagation, as predicted theoretically.

The above works mainly concern the propagation of Airy beams in free space. Up to now the following two studies seem to have been performed on the analysis of propagation of Airy beams in turbulence. The first belongs to Brooky and co-workers [8] who showed that Airy beam can retain its shape better than a Gaussian beam under laboratory simulated turbulence conditions. The second work in this area is due to Chu [9] who derived the moments of the Airy beam, and thereby investigating the evolution of intensity and kurtosis parameter of an Airy beam propagating in turbulence and free space.

In this paper, the propagation characteristics of a partially coherent Airy beam are investigated. Partial coherence is added because any practical source beam is partially coherent to a certain extent. Our aim is to see if such beams offer any advantages when they are used in horizontal optical communication links which is obviously dominated by turbulence.

2 Airy beam on source and receiver planes

Adopting one-dimensional representation for the source plane, the mutual coherence function of a partially coherent Airy beam covering two distinct points of the source plane can be written as follows:

$$T(s_{x1}, s_{x2}) = \text{Ai}\left(\frac{s_{x1}}{w_x}\right)\text{Ai}\left(\frac{s_{x2}}{w_x}\right)\exp\left[\frac{a_x(s_{x1} + s_{x2})}{w_x}\right]$$
$$\times \exp\left(-\frac{s_{x1}^2 + s_{x2}^2 - 2s_{x1}s_{x2}}{\sigma_c^2}\right) \tag{1}$$

where the parameter σ_c in the second exponential refers to the partial coherence property [10], while s_x is the coordinate along x axis. For identification purposes w_x is named the width parameter, a_x is on the other hand called the dislocation parameter, although both serve to alter the beam peak location as well as the source beam size, as will be demonstrated in the next section. Note that the form given in (1) already satisfies the square integrability condition mentioned in [2, 3]. The one-dimensional ensemble averaged intensity on a receiver plane situated at an axial distance of D away from the source can be calculated from the extended Huygens-Fresnel integral as

$$I(r_x) = \frac{k}{2\pi D}\int_{-\infty}^{\infty}\int_{-\infty}^{\infty}ds_{x1}ds_{x2}T(s_{x1}, s_{x1})$$
$$\times \exp\left[\frac{jk(s_{x1}^2 - s_{x2}^2 - 2r_xs_{x1} + 2r_xs_{x2})}{2D}\right]$$
$$\times \exp\left(-\frac{s_{x1}^2 + s_{x2}^2 - 2s_{x1}s_{x2}}{\rho_t^2}\right) \tag{2}$$

where k is the wave number related to source wavelength λ as $k = 2\pi/\lambda$ and $\rho_t = \left(0.546DC_n^2k^2\right)^{-3/5}$ is known to be the coherence length with C_n^2 being the structure constant, indicating the strength of turbulence. After inserting for $T(s_{x1}, s_{x1})$ in (2) from (1), it is possible to solve one of the double integrals in (2) using the following formulation

$$\int_{-\infty}^{\infty}dx\text{Ai}\left(\frac{x}{\varepsilon_1}\right)\exp\left(\frac{x}{\varepsilon_2}\right)\exp(ax^2 - bx)$$
$$= \left(-\frac{\pi}{a}\right)^{1/2}\text{Ai}\left(\frac{b}{2a\varepsilon_1} - \frac{1}{2a\varepsilon_1\varepsilon_2} + \frac{1}{16a^2\varepsilon_1^4}\right)$$
$$\times \exp\left(-\frac{b^2}{4a} + \frac{b}{2a\varepsilon_2} - \frac{1}{4a\varepsilon_2^2} + \frac{1}{8a^2\varepsilon_1^2\varepsilon_2} - \frac{b}{8a^2\varepsilon_1^3} - \frac{1}{96a^3\varepsilon_1^6}\right) \tag{3}$$

The resulting expression will then be

$$I(r_x) = \frac{k}{(2\pi D)^{1/2}}\left(-\frac{\rho_t^2\sigma_c^2}{C_d}\right)^{1/2}\exp\left(\frac{-6\rho_t^2\sigma_c^2Dw_x^4a_x^2C_d^2 + 6\rho_t^4\sigma_c^4D^2w_x^2a_xC_d - \rho_t^6\sigma_c^6D^3}{12w_x^6C_d^3}\right)$$
$$\times \int_{-\infty}^{\infty}ds_{x2}\text{Ai}\left(\frac{s_{x2}}{w_x}\right)\text{Ai}\left\{\frac{\rho_t^4\sigma_c^4D^2 - 8jk\rho_t^2\sigma_c^2Dw_x^3(s_{x2} + r_x)(\rho_t^2 + \sigma_c^2)}{4w_x^4C_d^2}\right.$$
$$\left. + \frac{8D^2w_x^2(\rho_t^2 + \sigma_c^2)[\rho_t^2\sigma_c^2a_x + 2w_xs_{x2}(\rho_t^2 + \sigma_c^2)] - 4k\rho_t^4\sigma_c^4w_x^2(kw_xr_x + jDa_x)}{4w_x^4C_d^2}\right\}\exp\left(\frac{a_xs_{x2}}{w_x}\right)$$
$$\times \exp\left[\frac{jk(-s_{x2}^2 + 2r_xs_{x2})}{2D} - \frac{(\rho_t^2 + \sigma_c^2)s_{x2}^2}{\rho_t^2\sigma_c^2}\right]\exp\left[\frac{C_p(2\rho_t^2\sigma_c^2Dw_x^2a_xC_d - w_x^3C_dC_p - \rho_t^4\sigma_c^4D^2)}{2\rho_t^2\sigma_c^2Dw_x^3C_d^2}\right] \tag{4}$$

where

$$C_d = jk\rho_t^2\sigma_c^2 - 2D(\rho_t^2 + \sigma_c^2),$$
$$C_p = jk\rho_t^2\sigma_c^2 r_x - 2Ds_{x2}(\rho_t^2 + \sigma_c^2). \quad (5)$$

By numerically evaluating the remaining single integral in (4), one can obtain the one-dimensional receiver intensity profile of Airy beam.

3 Graphical results and discussions

In this section, graphical outputs related to the formulations given in the previous and the present sections are provided. The numeric evaluations involve a single wavelength, which is $\lambda = 1.55$ μm. Additionally, unless stated otherwise, C_n^2 is taken as 10^{-15} m$^{-2/3}$ and coherence parameter σ_c is allowed to go to infinity. First the source plane intensity variations are explored with respect to dislocation and width parameters. For this purpose the source intensity can be retrieved from (1) as:

$$I(s_x) = \mathrm{T}(s_{x1} = s_x, s_{x2} = s_x) = \mathrm{Ai}^2\left(\frac{s_x}{w_x}\right)\exp\left(\frac{2a_x s_x}{w_x}\right). \quad (6)$$

Figure 1 shows the variation of the source intensity with a_x when w_x is held fixed at 1 cm. This figure reveals that a_x governs the dislocations of the beam peak such that the beam peak will drift along the s_x axis from negative side to the positive as a_x rises. Additionally, Fig. 1 demonstrates that rises in a_x values will eliminate the originally appearing oscillations of the negative axis and consequently the resulting sidelobes. Furthermore, these rises in a_x will initially reduce the magnitude of the beam peak, but when

switched to the positive side of the axis, the level of peaks will begin to rise again. Additionally, as detected from the profiles of $a_x = 1$ and 1.4, with rises in a_x, Airy beam will start to look more like a Gaussian beam. Our experiments have proven that, during propagation, such an Airy beam will also behave similar to a Gaussian beam. Tests show that the parameter a_x determines the location of the beam peak in relation to the values of the Airy function at zero argument in a manner that when

$$a_x < \frac{-\mathrm{Ai}'(0)}{\mathrm{Ai}(0)} = \frac{c_2}{c_1} = \frac{3^{-1/3}/\Gamma(1/3)}{3^{-2/3}/\Gamma(2/3)} \simeq 0.729 \quad (7)$$

the peak lies on the negative side of the s_x axis. The opposite occurs in other cases and the peak switches to the positive side. In (7), prime means differentiation with respect to the argument, $\Gamma(\ )$ refers to Gamma function and the coefficients c_1 and c_2 are the same as those given in [11]. Now, the changes in the source beam profile against w_x are investigated in Fig. 2, by fixing a_x to 0.2. As seen from Fig. 2, the beam will broaden with rising values of w_x, at the same time these rising values of w_x will leave the peak value at the same level, but cause it to drift toward the negative side of s_x axis. Here a_x is lower than the numeric value of 0.727, thus the peaks are inevitably placed on the negative side of the axis. Simple analytic exercise shows that, for given a_x, the peak will be located at s_x/w_x roots of

$$\mathrm{Ai}'\left(\frac{s_x}{w_x}\right) + a_x\mathrm{Ai}\left(\frac{s_x}{w_x}\right) = 0 \quad (8)$$

For small values of s_x/w_x, it is possible to take into account only the first few terms of the series expansion of Airy function supplied in [11] and then solve the resulting
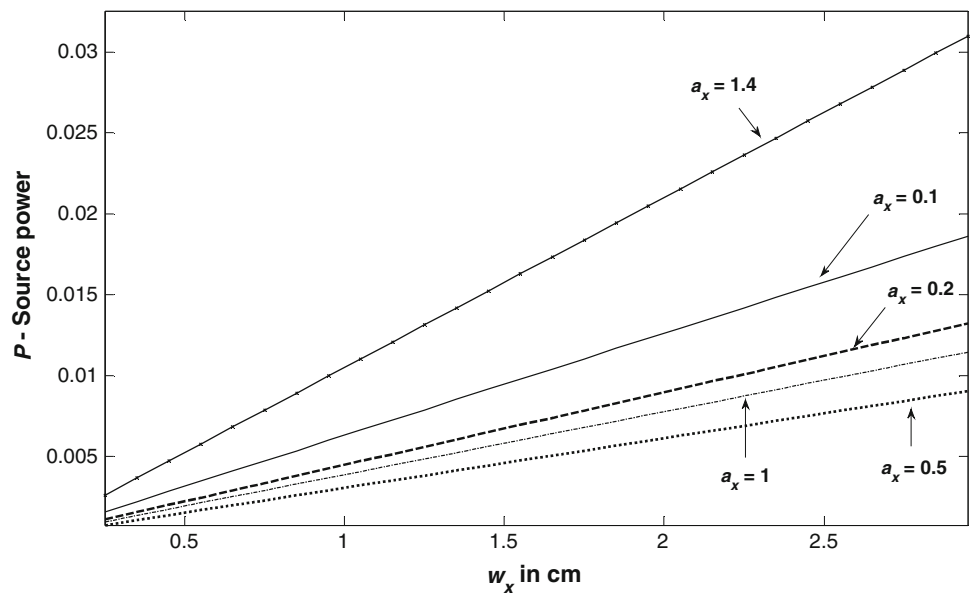

Fig. 1 Variation of source intensity profile with dislocation parameter (a_x) at constant width parameter of $w_x = 1$ cm
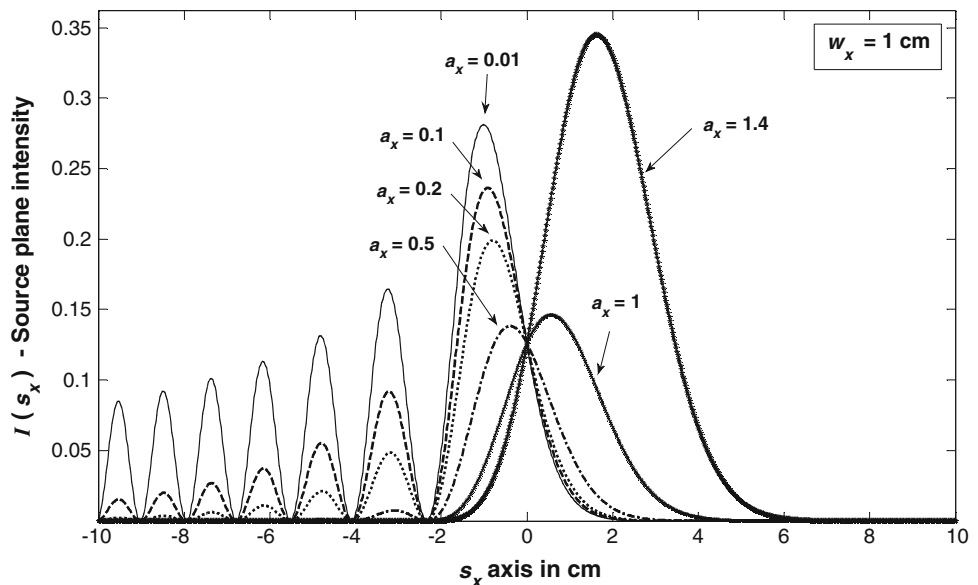
Fig. 2 Variation of source intensity profile with width parameter (w_x) at constant dislocation parameter of $a_x = 0.2$
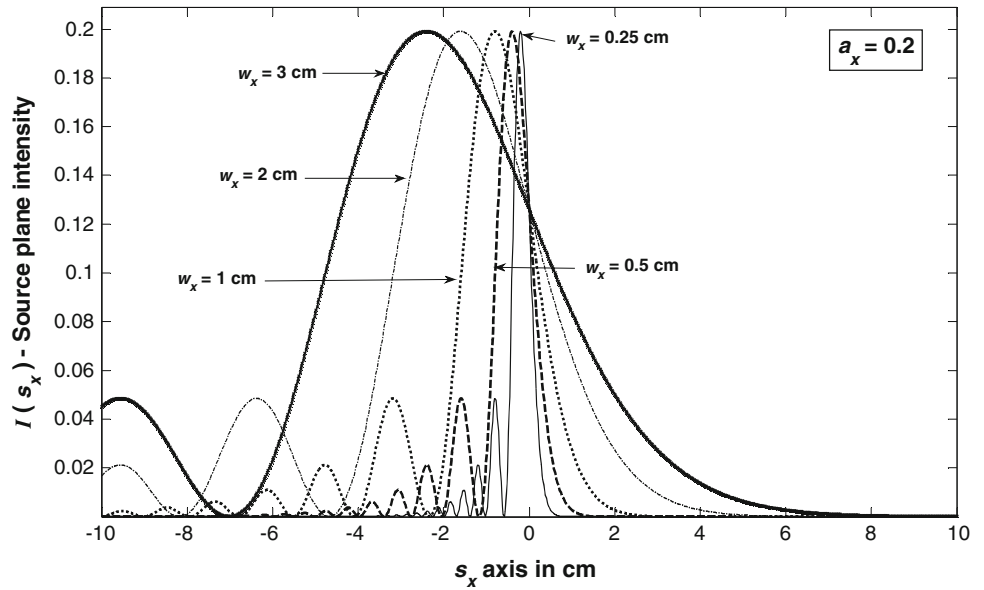
Fig. 3 Variation of source beam power against w_x at selected a_x values

polynomial equation using numerical methods. For larger values, the asymptotic expansions again given in [11] can be utilized. Relevant values obtained using this procedure are tabulated below.

a_x	Location of peak	Peak height, Max[$I(s_x)$]
0.1	$s_x/w_x = -0.94$	0.24
0.2	$s_x/w_x = -0.8$	0.2
0.5	$s_x/w_x = -0.39$	0.14
0.6	$s_x/w_x = -0.23$	0.13
0.8	$s_x/w_x = 0.14$	0.13
1	$s_x/w_x = 0.57$	0.15
1.4	$s_x/w_x = 1.63$	0.35

It can be said with comfort that the location of peaks, peak heights and other trends displayed in Figs. 1 and 2 with respect to w_x and a_x are well in agreement with the listings of the table above. The slight numeric discrepancies are due to employing a limited number of terms from the expansions.

It is obvious from Figs. 1 and 2, the changes in w_x and a_x essentially correspond to changes in the beam power and source beam size. Quantitatively, the one-dimensional source power contained in the Airy beam and the source beam size of the Airy beam along s_x axis can be derived from (6) as follows:

$$P = \int_{-\infty}^{\infty} ds_x I(s_x) = \int_{-\infty}^{\infty} ds_x \mathrm{Ai}^2\left(\frac{s_x}{w_x}\right) \exp\left(\frac{2a_x s_x}{w_x}\right) \qquad (9)$$

Fig. 4 Variation of source
beam size against w_x at selected
a_x values
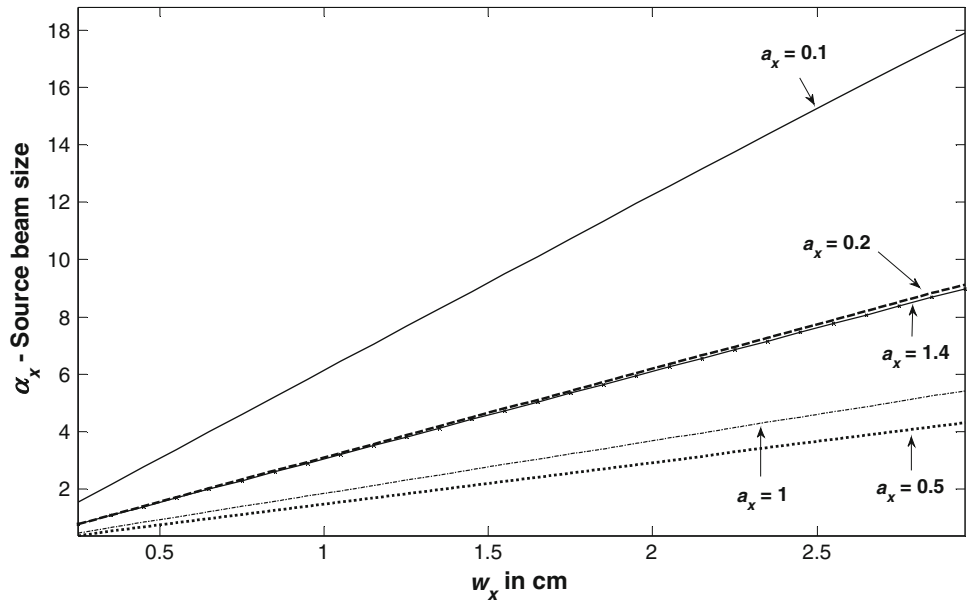
Fig. 5 Variation of receiver
intensity profile with
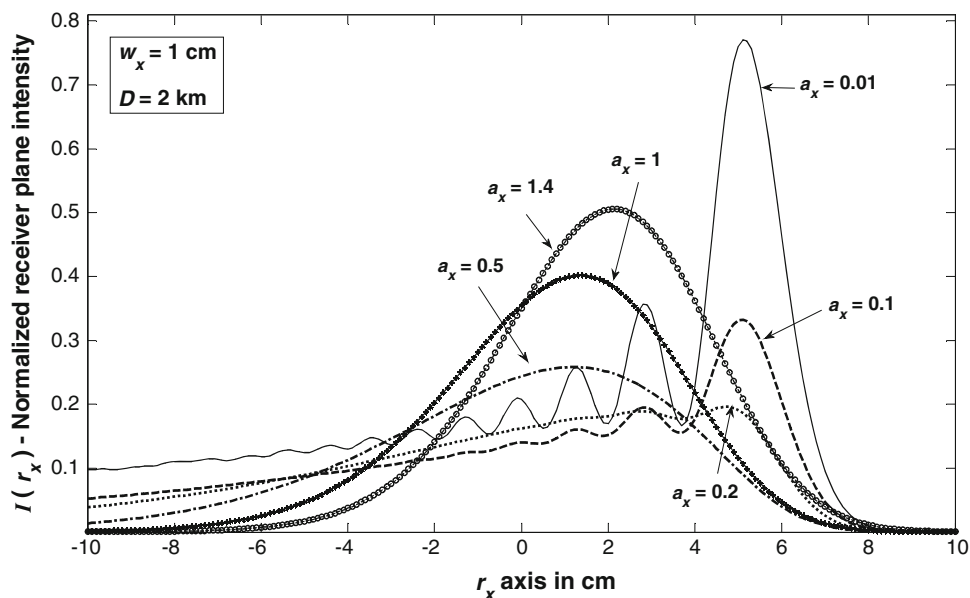propagation distance at constant
w_x and a_x
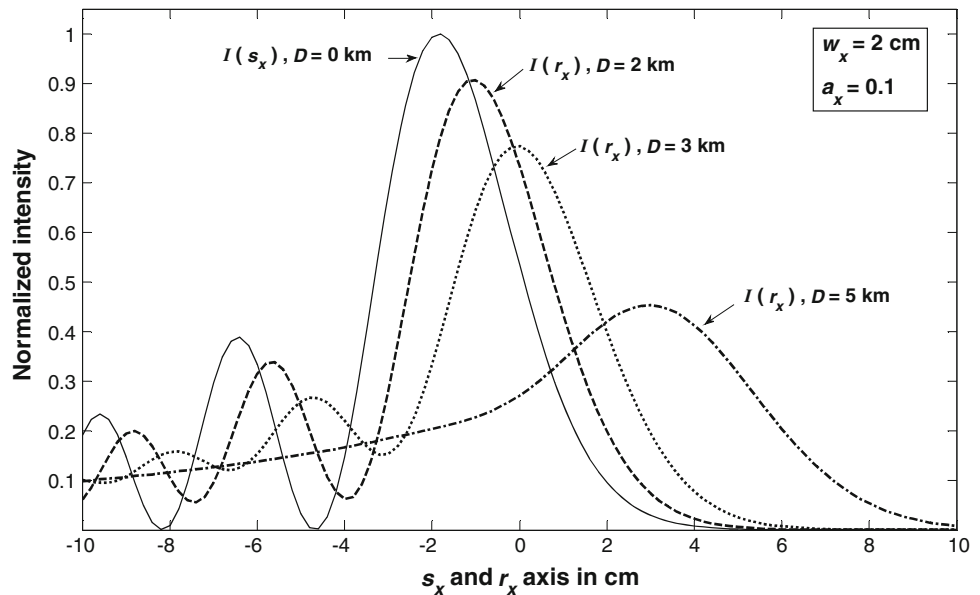
$$\alpha_x = \left[2 \int\limits_{-\infty}^{\infty} \mathrm{d}s_x s_x^2 I(s_x)/P \right]^{1/2} \tag{10}$$

Plotting the result of (9) against w_x at selective values of a_x as done in Fig. 3, it is seen that, more beam power, P will be obtained by increasing w_x, an observation in line with the one found in Fig. 2. The trend against increases in a_x is also similar to the one encountered in Fig. 1. That is, initially larger values of a_x will give smaller beams or beams with lesser power, while at a_x values exceeding 0.727, it will be possible to get larger beams, consequently beams with more power. Using (10), Fig. 4 shows the

variations of the source beam size against w_x at selective values of a_x. The curves in Fig. 4 have more or less the same behavior as those in Fig. 3 except, the Airy beam with $a_x = 0.1$ will continue to offer the largest source beam size throughout the examined range of w_x.

Next, the intensity profiles of the receiver plane are exhibited. In this context, Fig. 5 shows the intensity profiles at certain propagation distances including the one at $D = 0$, for fixed settings of w_x and a_x. It is clear from Fig. 5 that as the propagation distance is made larger, the beam will spread more, the oscillatory tails will smooth out. Due to the selection of a_x, the beam peak in Fig. 5 is initially located on the negative of the axis, but with increases in

**Fig. 6** Variation of receiver intensity profile with dislocation parameter at constant w_x and D

Fig. 7 Variation of receiver intensity profile with width parameter at constant a_x and D
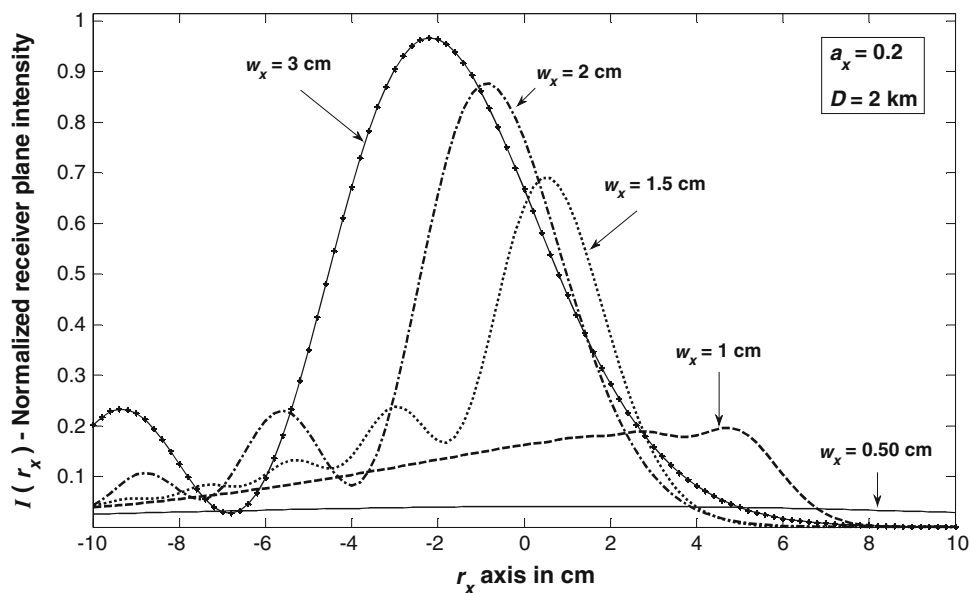
propagation distance, it will gradually switch to the positive side. It is imperative to realize that Fig. 5 illustrates the evolution of a single source beam against propagation distance, whereas Figs. 6 and 7 deal with the case of launching different beams from the source plane. This way, the effect of varying a_x on Airy beams at fixed w_x and D is shown in Fig. 6. Figure 7 on the other hand, displays the role of w_x on Airy beams upon propagation, this time at fixed a_x and D. In Fig. 6, it is seen that as a_x is made smaller the beam spreads more, while the peak location changes more rapidly to the positive side of the axis. It is clear from Figs. 2 and 4 that smaller w_x means reductions in the source beam size, hence in Fig. 7 the smaller values of w_x creating more

spreading and more accelerated beam evolution is quite reasonable [12]. Plots are also made by taking the other source beams of Figs. 1 and 2, but they are not included here to save space. Such plots reveal that the Airy beam will always bend towards the positive side of the transverse axis upon propagation independent of the initial location source beam peak. But these bends will become more like straight lines with increasing values of a_x and w_x. This is reasonable, since as seen from Figs. 1 and 2, with such increases, the main lobe of the source beam becomes larger and larger. These observations are partially in line with those of [13]. It is also possible to arrive at such deductions by establishing the free space equivalent expression of (4).

Fig. 8 Variation of receiver intensity profile with structure constant and partial coherence level at constant w_x, a_x and D
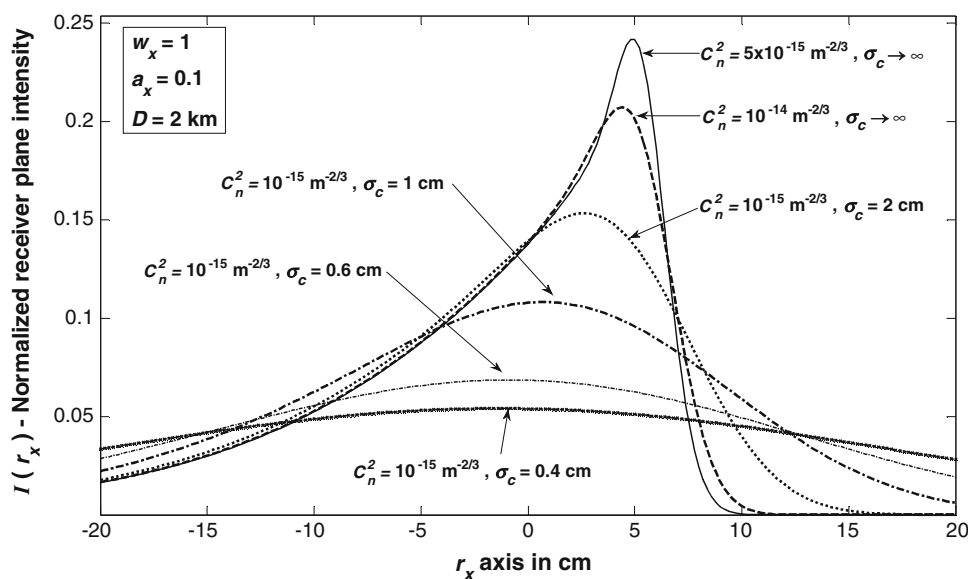
Finally the effects of structure constant and partial coherence parameters are analyzed and shown in Fig. 8. Accordingly, it is seen that both raising turbulence level by increasing the structure constant and adding more partial coherence to the source Airy beam by lowering σ_c will spread the beam more, although here the effect of partial coherence parameter seems to be more pronounced, as demonstrated by the curves of $\sigma_c = 0.6$ and 0.4 cm. Simultaneously such increases will also shift the beam peak more towards the on-axis position.

4 Concluding remarks

The properties of partially coherent Airy beam are analyzed on source and receiver planes. It is found that when on source plane, two parameters, namely dislocation and width parameters are jointly instrumental in shaping the beam profile and the location of the peak, although it is the numeric value of the dislocation parameter alone that determines whether the peak will lie on the positive or negative side of the transverse axis. Upon propagation, it is seen that the beam will spread out more and more with the oscillatory tails being smoothed out. And this process will accelerate with increasing propagation distance, structure constant and partial coherence level. Typically initially narrower Airy beams will evolve more rapidly. It is also seen that the beam will bend to the right during propagation, which means that the source beam whose peak is originally on the negative side of the axis can switch to the positive side. The amount of bending seems to be reduced with increasing values of dislocation and width parameters.

References

1. M.V. Berry, N.L. Balazs, Nonspreading wave packets. Am. J. Phys. **47**, 264–267 (1979)
2. G.A. Siviloglou, D.N. Christodoulides, Accelerating finite energy Airy beams. Opt. Lett. **32**, 979–981 (2007)
3. M.A. Bandres, J.C. Gutierrez-Vega, Airy-Gauss beams and their transformation by paraxial optical systems. Opt. Express **15**, 16719–16728 (2007)
4. Rui-Pin Chen, Hong-Ping Zheng, Chao-Qing Dai, Wigner distribution function of an Airy beam. J. Opt. Soc. Am. A **28**, 1307–1311 (2011)
5. S.N. Khonina, Specular and vortical Airy beams. Opt. Commun. **284**, 4263–4271 (2011)
6. D. Deng, H. Li, Propagation properties of Airy-Gaussian beams. Appl. Phys. B **106**, 677–681 (2012)
7. H.T. Dai, Y.J. Liu, D. Luo, X.W. Sun, Propagation properties of an optical vortex carried by an Airy beam: experimental implementation. Opt. Lett. **36**, 1617–1619 (2011)
8. J. Broky, G.A. Siviloglou, A. Dogariu, D.N. Christodoulides, Self-healing properties of optical Airy beams. Opt. Express **16**, 12880–12891 (2008)
9. X. Chu, Evolution of an Airy beam in turbulence. Opt. Lett. **36**, 2701–2703 (2011)
10. H.T. Eyyuboğlu, Propagation and coherence properties of higher order partially coherent dark hollow beams in turbulence. Opt. Laser Technol. **40**, 156–166 (2008)
11. M. Abramowitz, I.A. Stegun, *Handbook of Mathematical Functions* (Dover, New York, 1972)
12. H.T. Eyyuboğlu, Propagation of higher order Bessel-Gaussian beams in turbulence. Appl. Phys. B **88**, 259–265 (2007)
13. I.M. Besieris, A.M. Shaarawi, A note on an accelerating finite energy Airy beam. Opt. Lett. **32**, 2447–2449 (2007)